

Rewritable photonic circuits

Francesca Intonti,^{a)} Silvia Vignolini, Volker Türk, and Marcello Colocci
*European Laboratory for Non-Linear Spectroscopy, via N. Carrara 1, Sesto Fiorentino,
 Firenze, 50019 Italy*

Paolo Bettotti and Lorenzo Pavesi
Dipartimento di Fisica, Università di Trento, via Sommarive 14, Povo, Trento, 38050 Italy

Stefan L. Schweizer and Ralf Wehrspohn
Faculty of Science, University of Paderborn, Warburger Str. 100, 33098 Paderborn, Germany

Diederik Wiersma
*European Laboratory for Non-Linear Spectroscopy and INFM-CNR, via N. Carrara 1, Sesto Fiorentino,
 Firenze, 50019 Italy*

(Received 22 July 2006; accepted 5 October 2006; published online 22 November 2006)

The authors present a technique that allows to modify the local characteristics of two-dimensional photonic crystals by controlled microinfiltration of liquids. They demonstrate experimentally that by addressing and infiltrating each pore with a simple liquid, e.g., water, it is possible to write pixel by pixel optical devices of any geometry and shape. Calculations confirm that the obtained structures indeed constitute the desired resonators and waveguide structures. © 2006 American Institute of Physics. [DOI: 10.1063/1.2392720]

Along the way to all-optical devices in communication and information technology, photonic crystals (PCs) play a significant role. These structures, characterized by a periodic modulation of the refractive index that leads to the formation of a photonic band gap, a frequency range where light propagation in the crystal is forbidden,¹ form the basis material for the design and realization of several photonic applications, including complex waveguides,^{2,3} integrated microcavities,^{4,5} channel drop filters,^{6–8} optical switches,^{9,10} and low-threshold lasers.¹¹ By combining several of such elements the optical equivalent of an electronic circuit could in principle be obtained. A broad range of beautiful designs has been proposed but, so far, the experimental realization of such structures was technically very difficult and limited to simple elements such as missing pores, pores of different sizes and/or pores at different positions, incorporated at the growth stage of the photonic crystal. In this letter we present a powerful technique that allows to create such photonic circuits inside photonic crystals by controlled microinfiltration of liquid substances. With this technique it is possible to address and infiltrate each pore of a two-dimensional photonic crystal individually with a liquid of specific refractive index and nonlinear constant, with a local light source, and with liquid crystals in order to tune externally the refractive index.^{12–17} This technique enables the design and realization of various components and, above all, to combine several components into one single circuit. Another unique feature is that one can write both permanent structures and circuits that can be erased and rewritten.

Figure 1(a) shows a scheme of the experimental setup that we realized to implement the concept. The system is based on microinfiltration technology via hollow submicron size pipettes. Its practical realization requires a precise control of all the elements of the experimental setup, since the typical amount of liquid that has to be inserted in the pores of the photonic structure is of the order of 1 fl or less (about

three orders of magnitude smaller than the liquid droplets ejected by sophisticated ink jet printers). The infiltration process is monitored by a custom built confocal laser scanning microscope (CLSM) mounted on a commercial standard microscope (Zeiss, AxioTech) and equipped with a microinfiltration system (Eppendorf, Femtojet), developed for molecular applications, for transferring controlled amounts of liquid in cells. The microinfiltration system consists of a micropipette with an external diameter of less than 1 μm that can be moved with a precision of 0.1 μm on the sample surface. Hydraulic transmissions of the pipette movements strongly reduce vibrations. The actual infiltration is performed by bringing the tip of the pipette in close contact with the pore. The optical microscope is used to monitor the approach of the pipette to the sample surface and to choose the pore to be infiltrated. When the pipette gets in contact with the sample a light bending of the pipette is observed. In these conditions, if the pipette is moved on the sample plane, a hopping be-

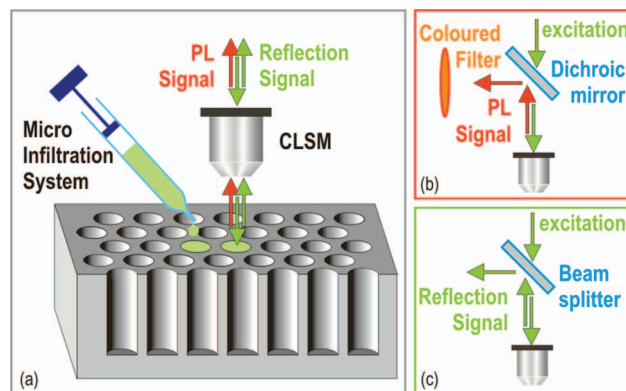


FIG. 1. (Color) Scheme of the experimental setup. (a) The controlled infiltration task is accomplished by a micro infiltration system and monitored with a CLSM that can work both in (b) luminescence configuration and in (c) reflection configuration. The possibility of switching between the two configurations, without changing the investigated area of the sample, is essential for controlling the successful infiltration at single pore level.

^{a)}Electronic mail: intonti@lens.unifi.it

havior is noticed, indicating that the pipette follows the sample topography. When the tip is in contact with the selected pore, an external pressure is applied to the pipette, which triggers the liquid infiltration.

Due to the submicron diameter of both the pipette and the to-be-infiltrated pore, capillary forces dominate the infiltration process. We observed that, even in a broad range of pressures applied to the pipette, successful infiltration takes place only if the liquid meniscus is in contact with the sample. Note that it is not necessary that the pipette enters the pore; it is sufficient that it just touches part of the pore walls. Since the actual infiltration is driven by capillary forces, we do not have a precise control of the amount of liquid that is inserted in the pore. The process appears self-regulating, terminating when the pore is completely filled. In all the samples that we have studied, we do not observe any problems connected with air trapped at the bottom of the pores, even in the case of pores that were closed on one side. A possible explanation for this is that the liquid flows along the pore walls during infiltration.

We chose to infiltrate a solution of water and the organic dye Rhodamine 6G. The chemical and physical properties of this solution appear particularly appealing for the proposed approach: (i) the refractive index of the aqueous solution is large enough, so that permitted states in the photonic band gap are introduced; (ii) its liquid viscosity is small enough to facilitate the deposition in the sample pores, and, at the same time, (iii) the liquid is not too volatile, in order to guarantee that the PC modification lasts in time; finally, (iv) it is possible to observe if the liquid has been exactly infiltrated in the pores, with a method alternative to standard microscopy. This last characteristic is important since the transferred liquid volumes are very small and yet should remain detectable. Once the solution is infiltrated in the pores, it acts as local defect, while the Rhodamine allows to investigate the spatial distribution of the solution by looking at the sample with the CLSM in luminescence configuration.

As the basis material in which to perform the infiltration, we chose periodic two-dimensional macroporous silicon which has been shown to behave as high quality two-dimensional photonic crystal.¹⁸ The samples on which we report here were characterized by triangular symmetry and had either a lattice constant of 4.2 or 1.5 μm .^{18,19} The silicon pore walls were all covered with a thin silicon oxide layer to allow wetting of the pores. Note that the infiltration experiments are not restricted to this material and can be transferred to any other system with the appropriate wetting properties.

Figure 2 shows a successful controlled infiltration at single pore level of the sample with smaller lattice constant. Figure 2(a) was recorded with the CLSM in emission configuration exciting at $\lambda=488$ nm, and collecting the luminescence signal of the Rhodamine solution [see Fig. 1(b)]. In order to block the excitation light, the CLSM is equipped with a dichroic mirror centered at 510 nm and a bandpass filter with transmission band from 520 to 560 nm that has a large overlap with the signal of the Rhodamine dissolved in water centered at 550 nm. Figure 2(b) was recorded in reflection configuration without changing the scanned region investigated in Fig. 2(a) by simply replacing the dichroic mirror with a standard 50/50 beam splitter and by removing the bandpass filter [see Fig. 1(c)]. Since the sample structure consists in air pores organized in triangular symmetry etched

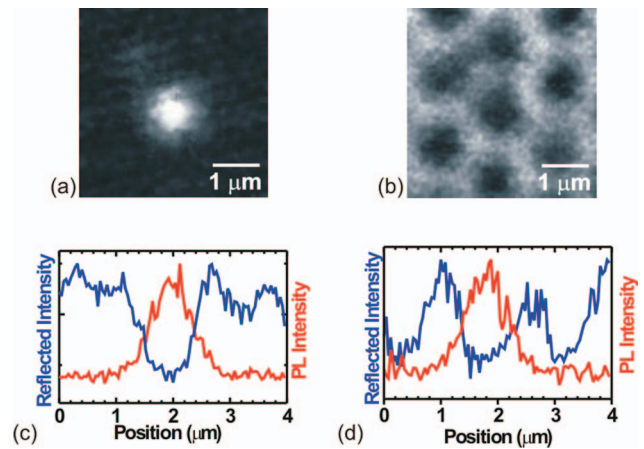


FIG. 2. (Color) (a) Luminescence signal: a single pore of 1 μm in diameter has been infiltrated with the Rhodamine solution. (b) Reflection image of the same sample region. (c) Horizontal and (d) vertical profiles along the center of the images in (a) and (b). The perfect overlap between the maximum in the luminescence curves (red lines) and the minimum in the reflection curves (blue lines) confirms that the solution is present only in the single selected pore.

in bulk silicon, the dark regions, indicating low reflectivity, correspond to the PC pores, while the light regions, indicating high reflectivity, coincide with the silicon veins between the air pores. The comparison between Figs. 2(a) and 2(b) confirms that the controlled infiltration was successful: the liquid has been introduced solely in the selected air pore. The horizontal and vertical profiles along the center of the two images, reported in Figs. 2(c) and 2(d), respectively, highlight that the position where in the first image there is a maximum in the signal, indicating the presence of the Rhodamine solution, corresponds exactly, in the reflection image to a minimum of the signal, that coincides with the position of the air pore.

The emission properties of organic dyes depend, in general, on the solvent in which they are dissolved and, in particular, once the water is evaporated the peak position shifts to 570 nm and gets a pronounced tail on the long wavelength side. By detecting this energy shift with opportune filters we can monitor the conditions and the time evolution of the intentionally introduced defects. When we collect the emission image after 24 h no substantial modifications are observed. However, the spatial distribution of the emission signal changes when the 520–560 nm bandpass filter is replaced with a low pass filter centered at 585 nm that has larger overlap with the emission associated with the dried Rhodamine signal. In this case the Rhodamine photoluminescence stems only from locations where by mistake tiny droplets of solution where accidentally deposited on the sample surface. From this observation we conclude that after 1 day has elapsed, inside the pores the Rhodamine is still in solution, while the liquid contents of the tiny droplets of solution accidentally deposited around the pores, on the sample surface, have evaporated. These small volumes of liquid evaporate rapidly if they are in free space or on top of a surface. Due to the high surface energy of the silicon oxide layer, capillary forces as well as wetting forces keep the liquid inside the pores and slow down the evaporation dramatically. This behavior presents a great advantage, both for studying the optical properties of intentionally inserted local defects and for future applications based on the presented

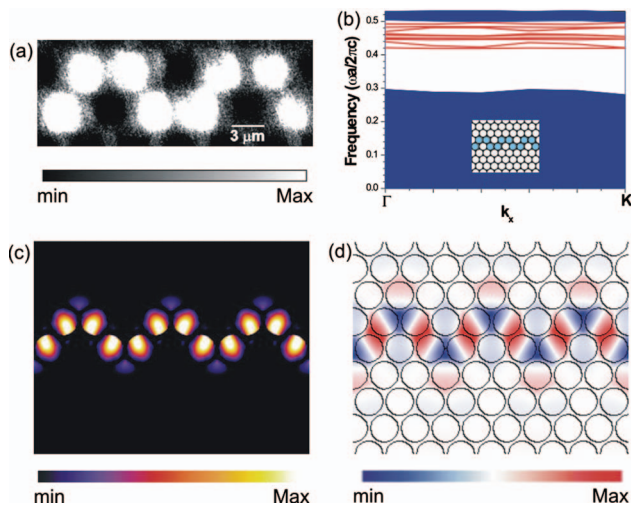


FIG. 3. (Color) Experimental realization of an “S-shaped” waveguide. (a) CLSM image collected in emission configuration in the sample region where successive microinfiltrations have created an “S4-waveguide.” (b) Calculated band diagram for the TE modes of the structure reported in the inset that simulates the experimental realized waveguide. The bulk sample is characterized by a band gap between $\lambda=0.3\omega a/2\pi c$ and $\lambda=0.5\omega a/2\pi c$. The inserted waveguide determines the appearance of a miniband of guided modes around $\lambda=0.45\omega a/2\pi c$. The inset reports the quasiperiodic variation of the dielectric constant that summarize the parameters chosen for simulating the S-shaped waveguide: pore radius, $r=0.45a$, water dielectric constant, $\epsilon(\text{H}_2\text{O})=1.77$, bulk dielectric constant, $\epsilon(\text{Si})=12$. The light blue spots represent the infiltrated pores. (c) Calculated spatial distribution of the electric field intensity associated with one of the TE mode introduced by the S-shaped waveguide inside the photonic band gap. (d) Calculated spatial distribution of the magnetic field associated with the same TE mode considered in (c).

idea of rewritable photonic devices. Any liquid can be completely removed by adding HF to the liquid to dissolve the silicon oxide layer, thereby converting the hydrophilic surface to a hydrophobic surface and successive heating, and/or by using an ultrasonic bath.

The limits of this technique on the minimum pore size are mainly determined by the size of the fiber tip and the optical resolution of the system used to monitor the infiltration process. Microtips as small as $0.5 \mu\text{m}$ are readily available and the limit to the tip diameter is today around $0.1 \mu\text{m}$. The optical resolution is diffraction limited to around 350 nm for deep-blue light, but this limit can be pushed further down by using UV light and charge-coupled device imaging. It should therefore be possible to infiltrate pores of around $200\text{--}600 \text{ nm}$ diameter, as typically encountered in photonic crystals in the $1.55 \mu\text{m}$ wavelength regime.

Having demonstrated the feasibility of the technique, we realized various structures. Figure 3 shows the results for an “S4 waveguide,” obtained by reiterating a building block of four infiltrated pores organized in a banded geometry. In Fig. 3(a) the luminescence signal from the infiltrated pores is shown. Figure 3(b) reports the calculated band diagram for the TE modes associated with this structure.²⁰ The blue regions correspond to propagating modes in the bulk crystal and the white region corresponds to the photonic band gap. The S4 waveguide introduces a miniband of guided modes (red curves) in the band gap.²¹ As shown in Figs. 3(c) and 3(d) the electromagnetic field associated with these modes is completely confined in the waveguide, demonstrating that the linear defect, introduced by the local infiltration of water, gives rise to an S-shaped waveguide in which light can

propagate without losses at the sharp bends. By addressing each pore individually one can also design and realize waveguides with different refractive indices in each hole, thereby creating, e.g., adiabatic bends with extremely small losses and solving the problem of impedance mismatching between components.

The presented technique based on controlled microinfiltration in porous photonic structures forms an enabling technology for the realization of all optical devices and circuits. Besides the increased flexibility in introducing defects of different types and natures, this approach offers the possibility of exactly tuning the energy resonance of the defect after fabrication by using a mixture of liquids of different refractive index. Since each pore of the photonic crystal can be addressed individually, these different materials can be combined to write either permanent or rewritable photonic circuits containing waveguides, active elements, and sources. Beyond integrated optics, the technique can be applied for any local infiltration application, e.g., to realize sensor chips by locally infiltrating a liquid that changes its optical properties when exposed to gas or biological species.

The authors thank Riccardo Sapienza and Roberto Righini for discussions and continuous support, Kurt Busch for discussions during the initiation of this project, and Pablo Cancio Pastor for help with the equipment. They acknowledge ITC-IRST for his support in microfabrication processes. This work was financially supported by the European Network of Excellence IST-2-511616-NoE (Phoremest), by EU Contract No. RII3-CT-2003-506350, and by the MIUR project Cofin 2004, Silicon Based Photonic Crystals.

¹E. Yablonovitch, *J. Opt. Soc. Am. B* **10**, 283 (1993).

²J. D. Joannopoulos, P. R. Villeneuve, and S. Fan, *Nature (London)* **386**, 143 (1997).

³A. Mekis, J. C. Chen, I. Kurland, S. Fan, P. R. Villeneuve, and J. D. Joannopoulos, *Phys. Rev. Lett.* **77**, 3787 (1996).

⁴J. S. Foresi, P. R. Villeneuve, J. Ferrera, E. R. Thoen, G. Steinmeyer, S. Fan, J. D. Joannopoulos, L. C. Kimerling, Henry I. Smith, and E. P. Ippen, *Nature (London)* **390**, 143 (1997).

⁵Y. Akahane, T. Asano, B. S. Song, and S. Noda, *Nature (London)* **425**, 944 (2003).

⁶S. Fan, P. R. Villeneuve, and J. D. Joannopoulos, *Phys. Rev. Lett.* **80**, 960 (1998).

⁷S. Noda, A. Chutinan, and M. Imada, *Nature (London)* **407**, 608 (2000).

⁸B. S. Song, S. Noda, and T. Asano, *Science* **300**, 1537 (2003).

⁹S. W. Leonard, H. M. van Driel, J. Schilling, and R. B. Wehrspohn, *Phys. Rev. B* **66**, 161102(R) (2002).

¹⁰X. Hu, Y. Liu, J. Tian, B. Cheng, and D. Zhang, *Appl. Phys. Lett.* **86**, 121102 (2005).

¹¹O. Painter, R. K. Lee, A. Scherer, A. Yariv, J. D. O’Brien, P. D. Dapkus, and I. Kim, *Science* **284**, 1819 (1999).

¹²K. Busch and S. John, *Phys. Rev. Lett.* **83**, 967 (1999).

¹³H. Takeda and K. Yoshino, *Phys. Rev. B* **67**, 073106 (2003).

¹⁴S. S. W. Leonard, J. P. Mondia, H. M. van Driel, O. Toader, S. John, K. Busch, A. Birner, U. Gösele, and V. Lehmann, *Phys. Rev. B* **61**, R2389 (2000).

¹⁵Y. Shimoda, M. Ozaki, and K. Yoshino, *Appl. Phys. Lett.* **79**, 3627 (2001).

¹⁶P. M. Johnson, A. Femius Koenderink, and W. L. Vos, *Phys. Rev. B* **66**, 081102(R) (2002).

¹⁷P. Halevi and F. Ramos-Mendieta, *Phys. Rev. Lett.* **85**, 1875 (2000).

¹⁸A. Birner, R. B. Wehrspohn, U. Gösele, and K. Busch, *Adv. Mater. (Weinheim, Ger.)* **13**, 377 (2001).

¹⁹P. Bettotti, L. Dal Negro, Z. Gaburro, L. Pavesi, A. Lui, M. Galli, M. Patrini, and F. Marabelli, *J. Appl. Phys.* **92**, 6966 (2002).

²⁰Calculations performed with code from S. G. Johnson and J. D. Joannopoulos, *Opt. Express* **8**, 173 (2001).

²¹A. Mekis, S. Fan, and J. D. Joannopoulos, *Phys. Rev. B* **58**, 4809 (1998).